ENVIRONMENTAL RESEARCH
LETTERS

LETTER • OPEN ACCESS

The impact of deforestation on rainfall in Africa: a data-driven assessment

View the article online for updates and enhancements.

ENVIRONMENTAL RESEARCH
LETTERS

CrossMark

LETTER

The impact of deforestation on rainfall in Africa: a data-driven assessment

Confidence Duku[1,2,*] and Lars Hein[1]

[1] Environmental Systems Analysis Group, Wageningen University, P.O. Box 47, 6700AA Wageningen, The Netherlands
[2] Wageningen Environmental Research, Climate Resilience Team, Wageningen University & Research, Wageningen, The Netherlands
* Author to whom any correspondence should be addressed.

E-mail: confidence.duku@wur.nl

Abstract

Forests play an important role in maintaining rainfall patterns worldwide by recycling water back to the atmosphere through evapotranspiration. We present a novel spatiotemporal data-driven model and assessment of the impacts of various deforestation scenarios on rainfall patterns in sub-Saharan Africa, where rainfed agriculture is the main source of income and provides food for a large part of the population. Our model is based on the convolutional long short term memory neural network and uses a combination of climate and vegetation time-series data to predict rainfall and to perform simulation experiments. Our results show that complete deforestation (i.e. conversion of all humid forests to short grasslands) would greatly reduce rainfall magnitude in the deforested areas. Above the equator, the large majority of areas not currently forested would also receive less rainfall. However, complete deforestation would slightly increase rainfall in some parts of Southern Africa and decrease it in other parts. The impacts of partial deforestation also differ across Africa. In West Africa, even moderate tree cover loss (i.e. 30%) reduces rainfall magnitude whereas in Central and Southern Africa, a threshold of 70% tree cover loss is required to reduce rainfall magnitude. Deforestation of remaining humid rainforest areas is thus likely to dramatically affect rainfed agriculture across the continent, in particular in the maize-based cropping systems north of the equator.

1. Introduction

There is increasing evidence that deforestation affects rainfall patterns (Lawrence and Vandecar 2014, Spracklen and Garcia-Carreras 2015, Van Noordwijk and Ellison 2019). Forests have evapotranspiration rates that are high compared to other ecosystems and thereby recycle rainfall back into the atmosphere where it becomes available to form clouds and forms new rainfall (Ellison *et al* 2017). In addition, forests affect cloud formation by releasing volatile organic compounds that form nuclei for raindrops (Kavouras *et al* 1998, Riccobono *et al* 2014). Finally, forests lead to local cooling, affecting turbulence and cloud formation (Li *et al* 2015). Consequently, the transformation of forests to other land-use types changes rainfall patterns. The effects of deforestation are noticeable at watershed to continental scales, with changes in forests in one country or watershed

potentially affecting rainfall in other countries or watersheds (Wang-Erlandsson *et al* 2018).

Deforestation has been forecasted to lead to lower rainfall in the Amazon (Salazar *et al* 2015), and has been linked to decreases in rainfall in eastern Australia (McAlpine *et al* 2009), Kalimantan (McAlpine *et al* 2018) and West Africa (Zeng 2003). However, for most of Africa, the effect of deforestation on rainfall has not yet been modelled, even though it has been postulated that deforestation in the western part of Central Africa affects rainfall in the Nile Basin (Gebrehiwot *et al* 2018). Across Africa, rainfall is derived from water evaporated in the Atlantic or Indian Ocean and the major lakes spread across the continent, or water resulting from evapotranspiration in Africa's humid ecosystems, in particular, the Central African rainforest. As elsewhere in the tropics, deforestation in Africa is rapid, and a major share of forests in West Africa have already been lost. In

relative terms, the forests of Central Africa, especially in the Democratic republic of Congo and the Republic of Congo have been comparatively well preserved (Hansen *et al* 2013, Keenan *et al* 2015). However pressure on sub-Saharan African forests, from among others smallholder and commercial agriculture, is rapidly intensifying (Ordway *et al* 2017, FAO, UNEP 2020). Given that a major share of Africa's population is dependent upon rainfed agriculture (Gassner *et al* 2019), it is crucial to better understand how African forests maintain rainfall patterns.

The objective of this paper is, therefore, to examine how sub-Saharan African forests maintain rainfall. Given the complexity of rainfall patterns and precipitationsheds, and the size of the African continent, we deployed a novel spatiotemporal machine learning approach, leveraging on remote sensing and climate reanalysis data to provide detailed insights into the relationship between forests and rainfall patterns. The development of the spatiotemporal machine learning model is a key novelty in our paper and is highly significant within the analysed range of deforestation (i.e. the model reflects very well the effects that deforestation has had on African rainfall to date). A second innovation is our focus on Africa, where there is an urgent need to clarify how ongoing land-use change may affect rainfall patterns.

2. Methodology

2.1. Input data and pre-processing
We developed a convolutional long short-term memory neural network (ConvLSTM) that predicts daily rainfall over the African continent using climate and vegetation input data. We regressed time-series of daily rainfall from 2000 to 2012 at a spatial resolution of 50×50 km covering the entire African continent against time series of daily wind speed and direction, net solar radiation, air pressure on the surface of the earth, evaporation from only water-bodies, tree cover and leaf area index (LAI) using the ConvLSTM (see next section). The covariates were selected to minimize multicollinearity. Specifically, we excluded atmospheric moisture contents from the covariates, because moisture is strongly correlated with rainfall, and including it masks the effects of changes in vegetation leading to changes in evapotranspiration rates and thereby atmospheric moisture. In effect, we masked evapotranspiration from land surfaces which is highly correlated to vegetation data, but we do include evaporation from oceans and large lakes. The rainfall data and climate covariates were obtained from the European Center for Medium-Range Weather Forecasts' Climate Reanalysis Data ERA-Interim reanalysis dataset (Dee *et al* 2011). Tree cover and LAI data were obtained from the moderate resolution imaging spectroradiometer at 250 and 500 m spatial resolutions respectively (Dimiceli *et al* 2015, Myneni *et al* 2015). The vegetation covariates

were realigned to the spatial and temporal resolution of climate covariates by computing the mean within 50×50 km and temporally downscaled to daily time-steps using fast Fourier transform (Cooley and Tukey 1965, Virtanen *et al* 2020).

2.2. Model setup and validation
The ConvLSTM that we developed is a variant of the long short-term memory neural network (LSTM). LSTMs are a type of recurrent neural network that have the capacity to learn long-term dependencies between input and output data (Hochreiter and Schmidhuber 1997). Unlike simple recurrent neural networks, LSTMs are able to retain information from longer sequence patterns. LSTMs, however, are limited to one-dimensional data and hence are unsuitable for spatiotemporal problems. The ConvLSTM addresses this limitation by replacing internal matrix multiplication with convolution operations (Shi *et al* 2015). The ConvLSTM has convolutional structures in both the input-to-state and state-to-state transitions. As a result, it preserves the three-dimensional spatial structure of input data. A ConvLSTM layer determines the future state of a grid cell based on the inputs and past states of the grid cell and its local neighbours. Like LSTMs, each ConvLSTM layer is made up of memory cells and three self-parameterized gates that control information flow. Equations (1)–(6) describe the generic details of a ConvLSTM layer (Shi *et al* 2015). Memory cells, C_t, accumulate information from input data over long periods of time. Forget gate, f_t determines which information stored in the previous cell state, C_{t-1}, would be discarded. Input gate, i_t, combines with a tanh layer, g_t, to update the previous cell state. Input gate determines which information stored in the previous cell state, C_{t-1}, would be updated and the tanh layer determines which candidate information from current input data, X_t, and previous output/hidden state, H_{t-1}, would be added to the memory cell. The output gate, o_t, determines which information from the current cell state, C_t, would be propagated to the current hidden state, H_t, and consequently will become candidate information to be accumulated in the cell state in the next sequence. The input, forget and output gates are composed of sigmoid functions, σ, ranging from 0 to 1, which determines the extent of information flow through the gates. For instance, if f_t equals 0, the model completely discards information stored in the previous cell state and if it equals 1 it retains all previous information. W is weight, which represents the strength of connection between units in each layer; b is bias, which is analogous to a constant in a linear function. $\odot$ denotes an element-wise dot product; $*$ denotes the convolution operator

$$i_t = \sigma \left(W_{i\_xi} * X_t + W_{i\_hi} * H_{t-1} + W_{i\_ci} \odot C_{t-1} + b_i \right), \tag{1}$$

$$f_t = \sigma \left(W_{f\_xf} * X_t + W_{f\_hf} * H_{t-1} + W_{f\_cf} \odot C_{t-1} + b_f \right), \tag{2}$$

$$o_t = \sigma \left(W_{o\_xo} * X_t + W_{o\_ho} * H_{t-1} + W_{o\_co} \odot C_t + b_o \right), \tag{3}$$

$$g_t = \tanh \left(W_{g\_xc} * X_t + W_{g\_hc} * H_{t-1} + b_c \right), \tag{4}$$

$$C_t = f_t \odot C_{t-1} + i_t \odot g_t, \tag{5}$$

$$H_t = o_t \odot \tanh \left(C_t \right). \tag{6}$$

We formulated the interaction between forests and rainfall patterns as a spatiotemporal regression problem, where the rainfall pattern (i.e. magnitude, duration and timing of peak rainfall) in a specific grid cell is not only determined by antecedent climatic and vegetation factors in that grid cell but also in the immediate neighborhood (3×3 neighborhood area). Our network structure consists of four stacked ConvLSTM layers sandwiched between two stacked convolutional neural network (CNN) layers and two stacked transposed convolutional (deconvolutional) layers. CNN's are specialized in image recognition and classification. They automatically learn a large number of convolutional filters, and apply these filters on input data resulting in feature maps, which indicate the locations and strengths of a series of detected features in the input data. First, the input data are fed into the CNN layers. The CNN layers transform the input data into a sequence of feature maps. This step is crucial because it reduces dimensionality of initial input data to more manageable groups for processing while at the same time largely preserving the spatial structure of input data. Second, the sequence of feature maps are fed into the stacked ConvLSTM layers, where actual spatiotemporal learning takes place. Finally, the transposed convolutional layers are applied to the output of the ConvLSTM layers to regain the spatial extent of the input data and to map the sequences of feature maps to a single output layer. For each time-step, the deconvolutional layers transform extracted feature maps into a single output layer representing the predicted rainfall at that time-step.

We evaluated the predictive accuracy of our model by dividing the sequential input data into training and test samples. The training sample contained sequential data from the beginning of the year 2000 to the end of 2012, whereas the test sample covered the beginning of 2013 to the end of 2015. The training sample was used by the neural network to approximate the relationship between input variables and rainfall. The test sample, however, was an independent data held out during the training process and which was used to evaluate the performance of the model.

2.3. Simulation experiments

We deployed the trained model to quantify effects of deforestation on rainfall using idealized deforestation experiments at two spatial scales i.e. whole agroecological region and individual pixels. In both simulation experiments, only vegetation input data were changed and climate input data remained the same. We assumed that changes in tree cover and LAI are unlikely to substantially affect surface net solar radiation, wind speed and direction and air pressure on the surface of the earth. First, we simulated the effects of large-scale complete and partial deforestation on rainfall patterns in the Guineo-Congolian region. In the complete deforestation scenario, tree cover and LAI dynamics in this region were fully replaced by short grassland whereas in the partial deforestation scenarios, tree cover in the Guineo-Congolian region was progressively reduced by 30%, 50% and 70%. The LAI sequences of the partial deforestation scenarios were computed using equation (7), where nLAI is the LAI after tree cover loss, gLAI is grassland LAI which is assumed to be the replacement vegetation after tree cover loss, coverLoss is the magnitude of tree cover lost (from 0 to 1), and fLAI is the LAI prior to tree cover loss

$$n\text{LAI} = g\text{LAI} * \text{coverLoss} + (1 - \text{coverLoss}) * f\text{LAI}. \tag{7}$$

In the Guineo-Congolian region, maximum daily LAI ranges from 6 to 9 and maximum tree cover is mostly above 50% whereas for short grassland, maximum tree cover is less than 1 and maximum LAI is less than 1. The trained model simulated the effects on rainfall magnitude, duration of the wet season and timing of peak period. These rainfall indicators were computed following Feng *et al* (2013) and using equations (8)–(12). For each year, the annual rainfall total, R_k, the associated monthly rainfall distribution, $p_{k,m}$, and the relative entropy, D_k are computed from the monthly total rainfall $r_{k,m}$ and where q_m is the uniform distribution, for which each month has a value of 1/12. Rainfall magnitude is calculated as annual rainfall total, R_k. The centroid, C_k, and spread, Z_k, representing the timing of peak rainfall and rainfall duration respectively are calculated using the first and second moments of $r_{k,m}$.

$$R_k = \sum_{m=1}^{12} r_{k,m}, \tag{8}$$

$$p_{k,m} = {r_{k,m}} / {R_k}, \tag{9}$$

$$D_k = \sum_{m=1}^{12} p_{k,m} \log_2 \left({p_{k,m}} / {q_m} \right) \tag{10}$$

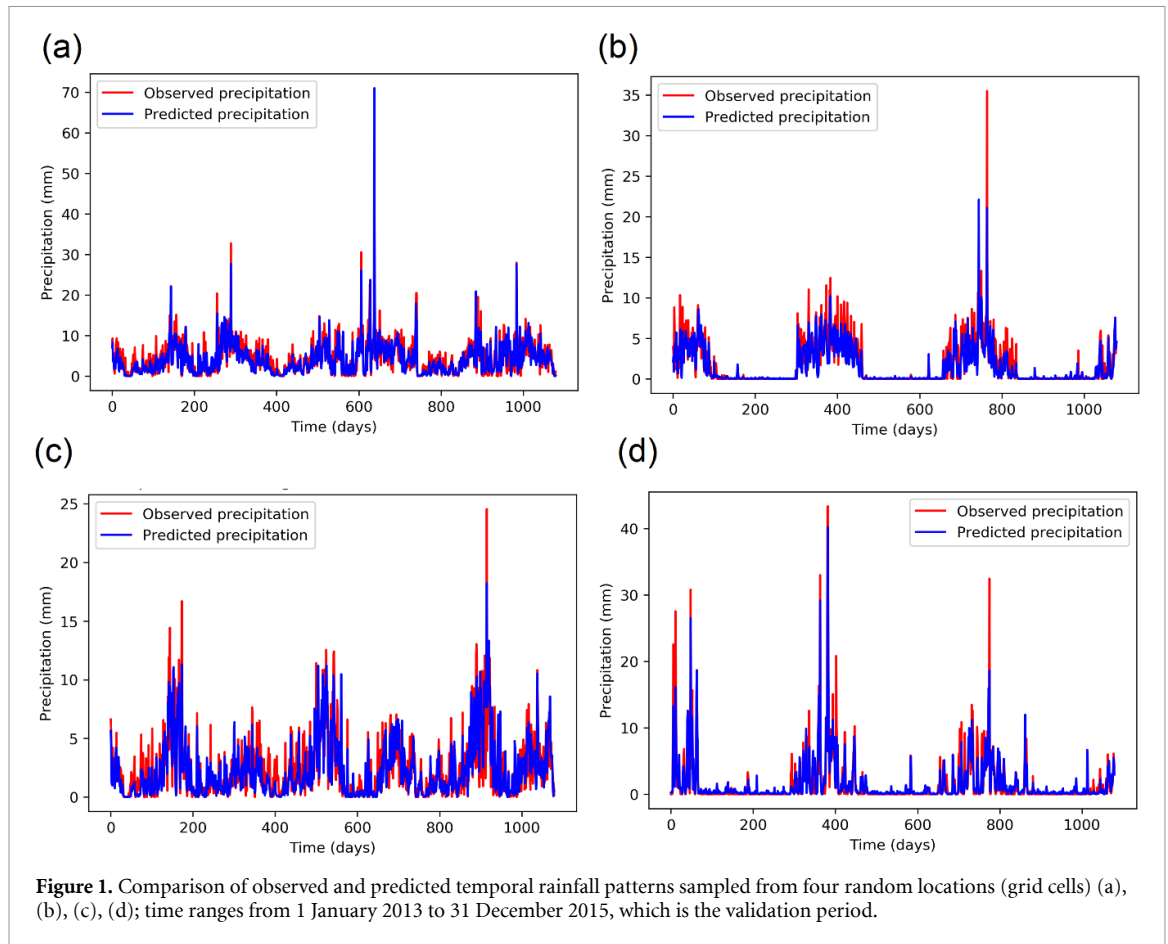$$C_k = \frac{1}{R_k} \sum_{m=1}^{12} m r_{k,m}, \tag{11}$$

Figure 1. Comparison of observed and predicted temporal rainfall patterns sampled from four random locations (grid cells) (a), (b), (c), (d); time ranges from 1 January 2013 to 31 December 2015, which is the validation period.

$$Z_k = \sqrt{\frac{1}{R_k} \sum_{m=1}^{12} |m - C_k|^2 r_{k,m}}. \qquad (12)$$

Second, for small-scale deforestation experiments, we sampled individual grid cells with high tree cover and LAI. Existing vegetation dynamics in these grid cells were replaced by short grassland vegetation dynamics.

3. Results

3.1. Model performance evaluation

We used a combination of statistical and graphical approaches to evaluate the predictive accuracy of the model. In general, our model can be considered highly accurate. Using the test sample for evaluation, the root mean squared error (RMSE), which is the aggregate magnitude of prediction errors across space and time, was 5.3 mm d^{-1}. The closer the RMSE is to 0.0, the better the absolute fit of the model. Based on the test sample, a percent bias (PBIAS) of -6% was recorded indicating that the model has the tendency to underestimate daily rainfall during peak rainfall events in the wet season. Given the low PBIAS, underestimation across space and time is either infrequent and/or not substantial. The model explains 75% of the variance in daily rainfall across space and time. Figures 1(a)–(d) presents a comparison of predicted and observed daily rainfall for four randomly selected pixels for different parts of Africa. It shows the tendency of the model to underestimate peak rainfall events. Figure 2(a) presents a scatterplot of predicted daily rainfall versus observed daily rainfall for all grid cells. It shows a high correlation between predicted and observed daily rainfall in most grid cells. The residual plot (i.e. difference between daily observed and predicted rainfall for each grid cell) presented in figure 2(b) shows that a substantial amount of grid cells had an error of 0 or close to 0. This result could be influenced by the large number of dry days in several grid cells. Even so, the results show that the model is able to predict dry days as well as wet days.

We also compared the spatial patterns of predicted and observed rainfall maps. Figure 3 shows how our predicted rainfall and observed rainfall align for mean monthly rainfall. Generally, predictive accuracy of the model increases from daily to annual rainfall. Nonetheless, the model adequately predicts the spatial pattern and dynamics of rainfall across Africa regardless of the time-step.

3.2. Effects of deforestation on rainfall patterns

The results clearly show that deforestation in the Guineo-Congolian region affects both local and remote rainfall magnitude, duration and timing of peak rainfall. The magnitude and direction of change,
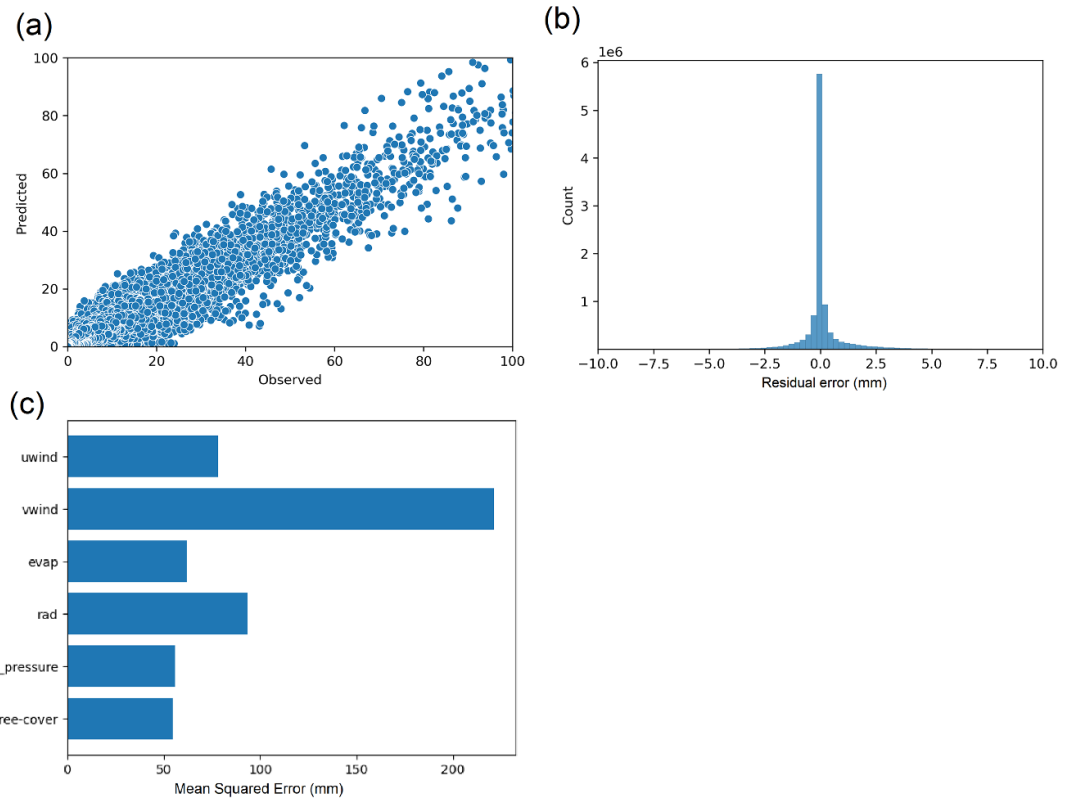
Figure 2. Model properties. (a) Scatterplot of observed and predicted daily rainfall—each dot compares observed and predicted rainfall from a single grid cell (50 × 50 km) for each day; (b) residual plot computed from difference between daily observed and predicted rainfall for each grid cell; (c) variable importance of input data. In (c), *uwind* is eastward or westward component of wind; *vwind* is northward or southward component of wind; *evap* is evaporation from only water surfaces including oceans and lakes; *rad* is net solar radiation; *surface_pressure* is atmospheric pressure on the earth's surface; and *lai + tree-cover* is the vegetation variable made up of tree cover and LAI. The mean squared error in the horizontal axis indicates the magnitude of prediction error from permuting a specific variable.
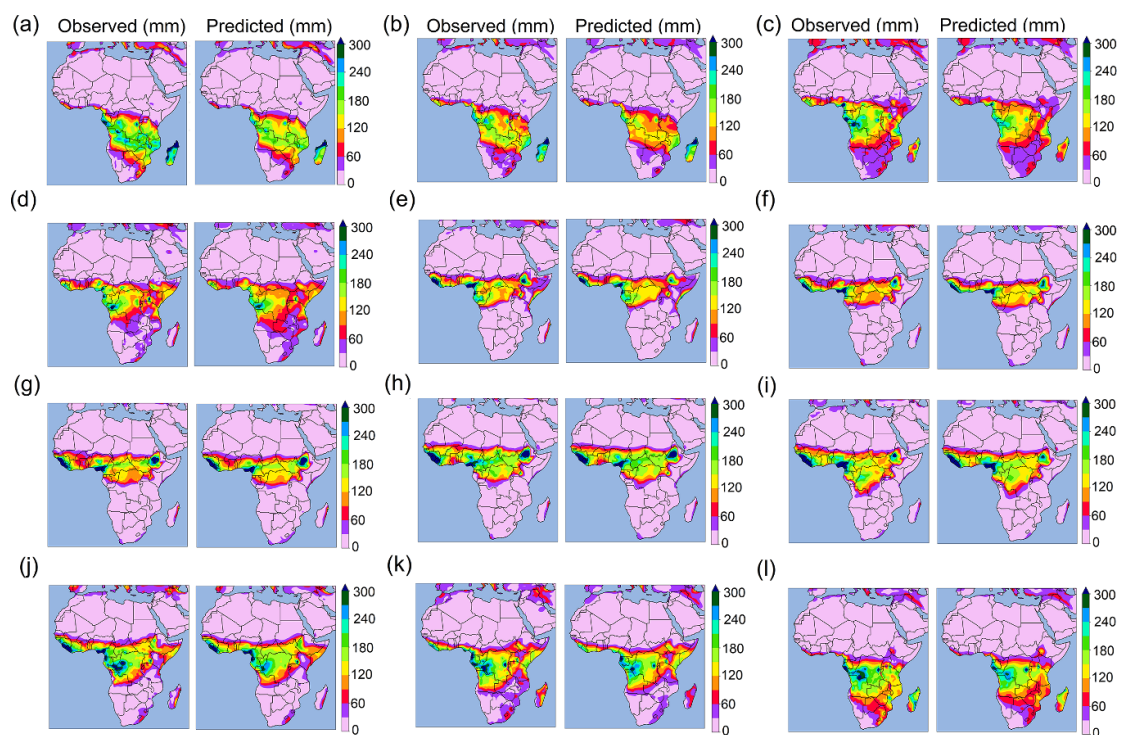

Figure 3. Comparison of observed and predicted mean monthly spatial rainfall patterns from January (a) to December (l). Monthly rainfall averaged over the validation period i.e. 2013–2015.
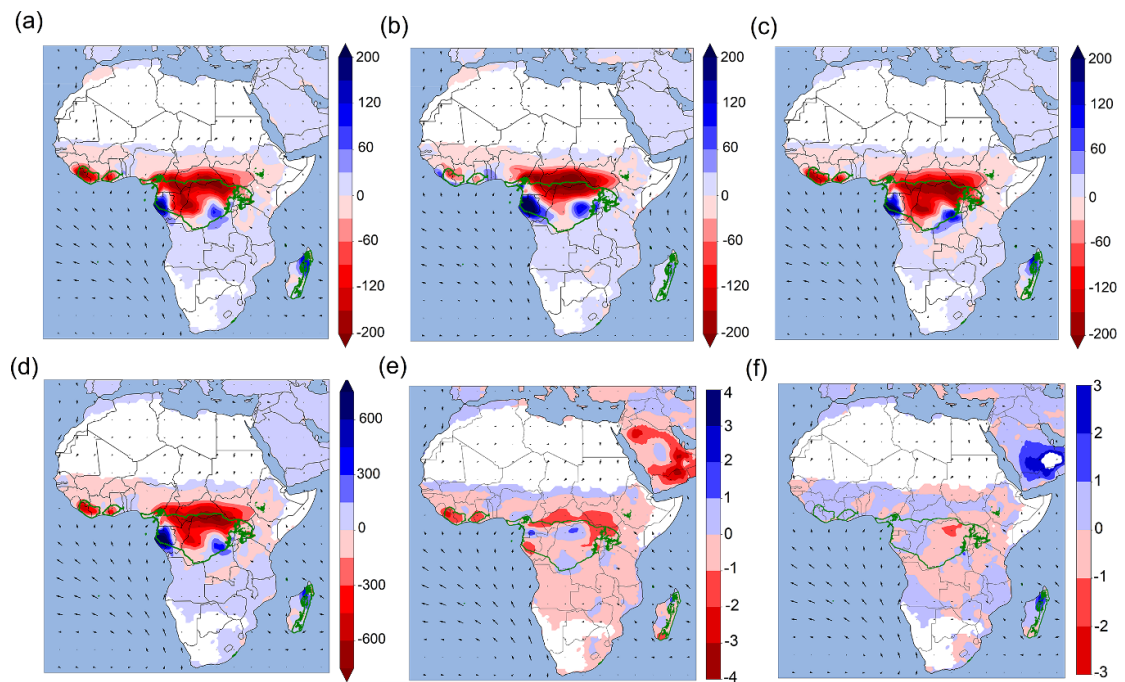
Figure 4. Changes in rainfall pattern as a result of complete deforestation in the Guineo-Congolian region. (a) Change in mean rainfall magnitude in the March–April–May season in mm season^{-1}; (b) change in mean rainfall magnitude in June–July–August season in mm season^{-1}; (c) change in mean rainfall magnitude in October–November–December season in mm season^{-1}; (d) change in mean annual rainfall magnitude in mm yr^{-1}; (e) change in mean duration of wet season in weeks; (f) change in timing of peak rainfall in weeks. For rainfall magnitude, negative values indicate reduction in rainfall and positive values indicate increase. For duration of rainfall, negative values indicate reduction in season length and positive indicate increase. For timing of peak rainfall, negative values indicate early onset of peak rainfall and positive values indicate delay. The green boundary indicates the Guineo-Congolian region, where deforestation was simulated. The black arrows indicate wind direction and speed.

however, vary depending on the proximity to deforested areas and the location with respect to wind direction. Figures 4(a)–(d) shows that conversion of forests and vegetation in the Guineo-Congolian region to short grassland reduces rainfall magnitude substantially in the deforested areas and in large areas above the equator, especially in West Africa below the Sahel. For instance, the Central African Republic and South Sudan would lose around 50% of their current average annual rainfall of about 1000 mm yr^{-1} (depending upon latitude). The Soudan-Sahel zone including Burkina Faso, southern Niger, southern Mali, northern Nigeria would lose around up to 40% of its annual rainfall. However, in Southern Africa, the picture is mixed, with some areas, in particular in the eastern part of the region, receiving more rainfall, and other areas receiving less rainfall.

Duration of the wet season and timing of rainfall are also likely to be affected by conversion of humid forests to grasslands. Figure 4(e) shows that the duration of the wet season will likely reduce as a result of deforestation in large areas of Africa. The worst affected areas will be in the deforested areas and/or the nearby areas where the wet season is likely to be reduced by up to 2 weeks. These include Central Africa Republic, South Sudan, Liberia and southwestern part of Ghana. Timing of peak rainfall will also delay in large areas in West Africa, whereas peak

rainfall would be early in large areas in Central Africa (figure 4(f)).

Our results also show that partial deforestation produces different responses across Africa (figure 5). In West Africa, tree cover loss and corresponding LAI reduction (irrespective of the magnitude of loss) within the Guineo-Congolian region consistently reduce rainfall magnitude. The greater the tree cover loss the greater the reduction in rainfall magnitude. This indicates that West African countries, especially, depend more on recycled evapotranspiration for rainfall. This is more evident during the West African dry seasons compared to wet seasons. For example, in the deforestation simulation experiments, the magnitude and spatial extent of rainfall reduction in the June–July–August season (the wet season) is considerably lower than in the March–April–May and October–November–December seasons (see figure 5). In Central and Southern Africa, however, 50% tree cover loss (or less) increases rainfall magnitude in most deforested areas during all seasons. Rainfall reduces only after a threshold of 70% reduction in tree cover.

To examine if our model can also be used in support of efforts to account for the various services provided by forests (e.g. Hein *et al* 2020), we simulated the effects of conversion of specific forested grid cells (50 × 50 km) to short grasslands. These grid cells were selected in areas with high deforestation
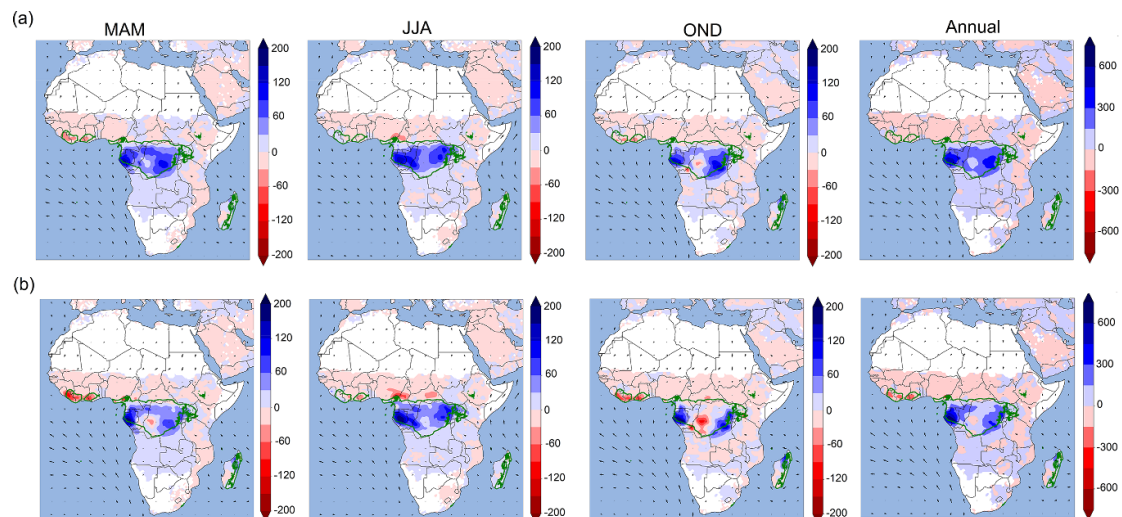
Figure 5. Changes in rainfall magnitude as a result of partial deforestation in the Guineo-Congolian region. (a) Change in mean rainfall magnitude as a result of 50% tree cover loss during the simulation period; (b) change in mean rainfall magnitude as a result of 70% tree cover loss. MAM refers to the March–April–May season, JJA refers to the June–July–August season and OND refers to the October–November–December season. The green boundary indicates the Guineo-Congolian region, where deforestation was simulated. The black arrows indicate wind direction and speed.
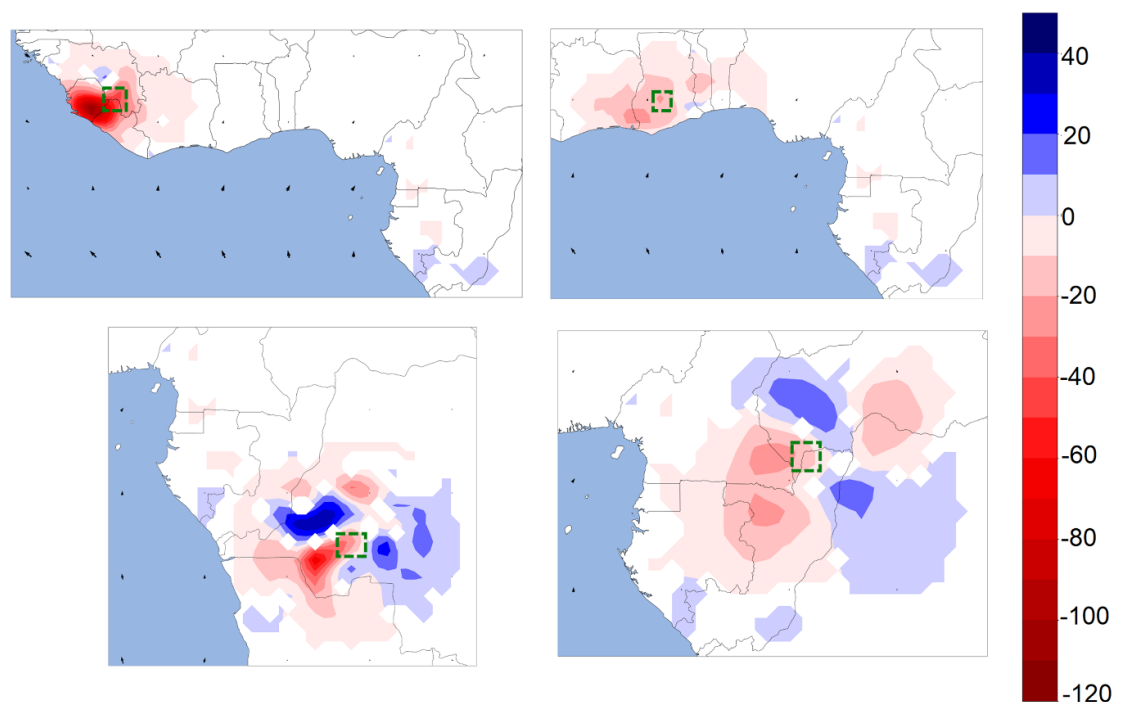

Figure 6. Change in mean annual rainfall magnitude (mm yr^{-1}) as a result of complete deforestation in individual grid cells. The green dashed boxes indicate areas where deforestation was simulated. The black arrows indicate annual average wind direction and speed.

rates (e.g. West Africa and Central Africa). Figure 6 shows that in West Africa, local deforestation consistently reduces rainfall magnitude in the deforested location and the immediate neighboring areas. However, in Central Africa, it decreases rainfall locally and increases rainfall, to a lesser extent, in remote locations. For example, local deforestation in northern Liberia, reduces rainfall by about 80 mm yr^{-1} in the north-west of Liberia as well as large areas of Sierra

Leone. But rainfall in the Central Africa increases by about 10 mm yr^{-1} (figure 6).

4. Discussion

4.1. Uncertainties and limitations of the approach
As with any modelling approach, and in particular a data-driven continental scale model, there are uncertainties and limitations in the model that we

developed. A first point is that the model analyses changes in rainfall patterns as they have occurred in the period 2000–2015, and extrapolates the correlation between deforestation and rainfall to the future with a forest cover much lower than experienced in the period 2000–2015. This effect, of course, is particularly relevant for the scenario where we deforest all humid tropical forests of Africa and replace them with short grassland, and less so for the analysis where we deforest a single pixel (50 × 50 km) in order to assess impacts on rainfall. In the first case, the replacement forest cover that we analyse is quite distinct from the set of forest covers that we used as model inputs. Consequently, our forecast of how rainfall would change as a function of complete deforestation should be seen as illustrative— showing a first estimate of the potential consequences of the loss of African forests. A process-based ocean–atmosphere–land surface model (e.g. McAlpine *et al* 2009) could be more accurate in representing impacts of forest losses that far exceed current deforestation patterns. However, configuring a process-based ocean–atmosphere–land surface model at the scale of Africa, with hydrological cycles and wind patterns modelled at daily time-steps is challenging given the number of parameters that would need to be calibrated. Moreover, even in case of process-based models the model parameters need to be estimated based on rainfall and hydrological processes as they currently occur, and there will be substantial uncertainty when the model is used to forecast rainfall under strongly different forest covers. Hence, we believe our current modelling approach is currently the best possible option given data and computing limitations. Improvements of our model could focus on increasing spatial resolution of climate and vegetation data to better capture local spatiotemporal processes. Increasing spatial resolution, however, considerably affects computational efficiency and would require considerable increases in computational resources for processing and data storage. The use of extensive vegetation data beyond LAI and tree cover can also better capture vegetation-climate interaction and feedbacks. However, consistent and spatially-explicit time-series data needed are mostly unavailable for Africa.

Furthermore, our paper did not address feedbacks in ecosystem dynamics (e.g. Scheffer *et al* 2001). With increasing deforestation, positive feedbacks (with negative societal consequences) may occur. For instance, reduced rainfall generally increases fire risks (Hoffmann 2003). Increased fire risks may further exacerbate pressure on forests leading to further reductions in forest cover, in particular, in sub-humid conditions. Since we do not consider such feedbacks in our analysis, we may underestimate the effects of deforestation on rainfall patterns.

4.2. Modelling forest-rainfall relationships

Our paper presents the impacts of an extreme scenario, because some of the forests are protected and also because the current land-use change is in part to plantations, which have a higher evapotranspiration rate than short grasslands and therefore lead to a somewhat lower impact on rainfall patterns. Nevertheless, in earlier work the effects of deforestation have also been demonstrated using extreme deforestation scenarios. Our results can be compared with those of Abiodun *et al* (2008) who deploy the International Centre for Theoretical Physics Regional Climate Model and find that extreme deforestation reduces average monsoon rainfall across West Africa with approximately 50–400 mm yr^{-1}. These values are higher than what we find, but we note that their scenario also involves deforestation in the sub-humid forests of West Africa. Zheng and Eltahir (1997), in an older paper, even find that the monsoon collapses in West Africa should all tropical forests be replaced by savannah vegetation. Our results are also well aligned, both in terms of magnitude and spatial patterns, with Semazzi and Song (2001), who model the effects of replacing tropical rainforest with savanna grassland with the National Center for Atmospheric Research CCM3 global climate model. They find rainfall reductions in deforested areas with 2–3 mm d^{-1} in July–September and less than 1 mm d^{-1} during the wetter autumn and spring months. Similar to our results, they find that deforestation results in substantial rainfall reduction over Mozambique but a rainfall increase in other parts of Southern Africa, connected to changes in the trapped Rossby wave train activity generated by the mid-tropospheric latent heating over the tropical forest region (McIntosh and Hendon 2018). Over Central and West Africa, the impact of deforestation is primarily characterized by a reduction in rainfall (Semazzi and Song 2001). We conclude that our results, although derived in an entirely different way (using machine learning instead of global climate model), are comparable to the relatively few studies using global and regional climate models to assess the effects of deforestation in Africa.

4.3. Policy implications

It is clear that deforestation affects rainfall (e.g. McAlpine *et al* 2009, McAlpine *et al* 2018, Salazar *et al* 2015). Our paper shows that also in Africa deforestation will have major consequences for rainfall patterns. In general terms, deforestation has been severe in most West African countries (Hansen *et al* 2013, CILSS 2016), and is still continuing, for instance, in Ivory Coast where forests are still converted to, among others, cocoa plantations (Barima *et al* 2016). The Central African rainforest is still relatively well-preserved, perhaps thanks to institutional and safety challenges that occur in the two Congo's. Nevertheless, deforestation continues across Africa, for

instance in Tanzania and Zambia (Hansen *et al* 2013), both as a consequence of large scale land conversion and due to smallholders establishing new farms and wood harvesting for firewood and charcoal production. To date, many policy makers in Africa do not see this as a serious concern, instead assuming that forest loss is an acceptable part of economic development.

However, this paper shows that deforestation will have major economic consequences for Africa. In Africa, a large proportion of the population is dependent upon rainfed agriculture (Gassner *et al* 2019). For instance, maize-based farming systems are spread across Africa and provide food to some six to seven hundred million people (Dixon *et al* 2001, Van Ittersum *et al* 2016). Productivity of these systems is constrained by water, and water shortages in dry years tend to lead to crop failures. Climate change is expected to reduce rainfall and increase temperatures in large parts of Africa, reducing the growing season (e.g. Duku *et al* 2018). At the same time, the population of Africa is expected to double between now and 2050 (UN 2019). Hence, reductions in rainfall patterns due to deforestation could have severe economic and food security implications that urgently need to be acknowledged in policy making.

Policy-making should also consider that the forest-rainfall relationship is not always monotonic and critical thresholds exist which, together with teleconnection effects, call for transnational or regional cooperation in forest management. For example, our paper has shown that recycled evapotranspiration from Central African humid forests (in addition to the remaining humid forests in West Africa) is a substantial component of rainfall in water-scarce West Africa. Even moderate tree cover loss in Central Africa thus reduces rainfall in West Africa. However, over the deforested locations in Central Africa itself, our model predicts that only tree cover loss above 70% reduces rainfall. These different rainfall responses go to show that specific effects depend on both local and remote characteristics, and that these effects are non-linear. Finally, our paper shows the importance of considering the service 'maintaining rainfall patterns' in ecosystem services studies including those of the Intergovernmental Science-Policy Platform on Biodiversity and Ecosystem Services and the System of Environmental Economic Accounting—Ecosystem Accounting (e.g. Hein *et al* 2020). This service is underestimated—it is not usually included in either ecosystem services assessments or accounting efforts. Our paper lays out a potential approach to map and quantify the specific contribution of forest areas for maintaining rainfall patterns, thereby allowing their mapping and inclusion in assessment and accounts. In this context it is relevant to stress the importance of scale: for example, the impact on rainfall patterns of 1 hectare of forest, will not be picked up by a continental or even sub-continental scale model. However, the impacts of deforestation of one grid cell in our model (2500 km^2) are noticeable, as illustrated in figure 6. Further discussions are required to assess if it would be reasonable, for the purpose of accounting for the services provided by forests, to downscale this impact measured in a 2500 km^2 grid cell to smaller grid cells, and if so how this downscaling can best be done.

5. Conclusions

Our paper shows that, as in other continents, forests in Africa are essential to sustain rainfall patterns. Arguably, the service is even more important in Africa than in any other place in the world because the continent has vast agricultural zones that are dependent upon secondary rainfall (i.e. rainfall not generated from evaporation in oceans), a large and growing population for which rainfed agriculture is the main source of income and food, and extensive areas that are already constrained in cropping potential by low rainfall. Unfortunately, there is as yet very little consideration of this key ecosystem service provided by African forests in policy and decision making. This paper shows that complete deforestation (i.e. conversion of humid forests to short grasslands) greatly reduces rainfall magnitude in the deforested areas. In remote locations, complete deforestation reduces rainfall magnitude in areas above the equator whereas large areas below the equator experience slight increases in rainfall magnitude. The worst affected areas are likely to be the Central African Republic and South Sudan, where about 50% of annual rainfall will be lost if the Central African humid forests would be converted to grassland. The Soudan-Sahel zone in West Africa would lose up to 40% of its annual rainfall in the extreme scenario of complete forest loss. Complete deforestation would also lead to a reduction in the duration of the wet season with the worst affected areas experiencing a reduction of up to 2 weeks. Partial deforestation, however, produces differing rainfall responses in the deforested areas of West and Central African humid rainforests. In West Africa, even moderate tree cover loss (i.e. 30%) reduces rainfall magnitude whereas in Central Africa, a threshold of 70% loss of remaining tree cover is required to reduce rainfall magnitude. Below this threshold, tree cover loss in Central Africa increases rainfall magnitude. Hence, it is of paramount importance to recognize the dependency of African rainfed agriculture, especially cropland areas above the equator and in West Africa, on forest conservation, and to protect remaining forests in order to safeguard farmers' livelihoods.

Data availability statement

The data that support the findings of this study are openly available at the following URL/DOI: https:// lpdaac.usgs.gov/products/mod44bv006/.

ORCID iD

Confidence Duku ⬤ https://orcid.org/0000-0002-1670-3451

References

Abiodun B, Pal J, Afiesimama E, Gutowski W and Adedoyin A 2008 Simulation of West African monsoon using RegCM3 part II: impacts of deforestation and desertification *Theor. Appl. Climatol.* **93** 245–61

Barima Y S S, Kouakou A T M, Bamba I, Sangne Y C, Godron M, Andrieu J and Bogaert J 2016 Cocoa crops are destroying the forest reserves of the classified forest of Haut-Sassandra (Ivory Coast) *Glob. Ecol. Conserv.* **8** 85–98

CILSS 2016 Landscapes of West Africa—a Window on a Changing World *CILSS:. Comité Permanent Inter-états de Lutte contre la Sécheresse* (Burkina Faso: dans le Sahel Ouagadougou)

Cooley J W and Tukey J W 1965 An algorithm for the machine calculation of complex Fourier series *Math. Comput.* **19** 297–301

Dee D P et al 2011 The ERA-Interim reanalysis: configuration and performance of the data assimilation system *Q. J. R. Meteorol. Soc.* **137** 553–97

Dimiceli C, Carroll M, Sohlberg R, Kim D, Kelly M and Townshend J, 2015. MOD44B MODIS/Terra vegetation continuous fields yearly L3 global 250 m SIN grid V006. *NASA EOSDIS Land Processes Distributed Active Archive Center*

Dixon J, Gulliver A, Gibbon D and Hall M 2001 *Farming Systems and Poverty: Improving Farmers' Livelihoods in a Changing World* (Washington, DC: World Bank Group)

Duku C, Zwart S J, Van Bussel L G J and Hein L 2018 Quantifying trade-offs between future yield levels, food availability and forest and woodland conservation in Benin *Sci. Total Environ.* **610–611** 1581–9

Ellison D et al 2017 Trees, forests and water: cool insights for a hot world *Glob. Environ. Change* **43** 51–61

FAO, UNEP 2020 The State of the World's Forests 2020 *Forests, Biodiversity and People* (Rome: Food & Agriculture Organization of the United Nations, United Nations Environmental Programme) 82–5

Feng X, Porporato A and Rodriguez-Iturbe I 2013 Changes in rainfall seasonality in the tropics *Nat. Clim. Change* **3** 811–5

Gassner A, Harris D, Mausch K, Terheggen A, Lopes C, Finlayson R F and Dobie P 2019 Poverty eradication and food security through agriculture in Africa: rethinking objectives and entry points *Outlook Agric.* **48** 309–15

Gebrehiwot S G, Ellison D, Bewket W, Seleshi Y, Inogwabini B I and Bishop K 2018 The Nile Basin waters and the West African rainforest: rethinking the boundaries *Wiley Interdiscip. Rev.* **6** e1317

Hansen M C et al 2013 High-resolution global maps of 21st-century forest cover change *Science* **342** 850–3

Hein L et al 2020 Progress in natural capital accounting for ecosystems *Science* **367** 514–5

Hochreiter S and Schmidhuber J 1997 Long short-term memory *Neural Comput.* **9** 1735–80

Hoffmann W A 2003 Regional feedbacks among fire, climate, and tropical deforestation *J. Geophys. Res.* **108** 4721

Kavouras I G, Mihalopoulos N and Stephanou E G 1998 Formation of atmospheric particles from organic acids produced by forests *Nature* **395** 683–6

Keenan R J, Reams G A, Achard F, De Freitas J V, Grainger A and Lindquist E 2015 Dynamics of global forest area: results from the FAO Global Forest Resources Assessment 2015 *For. Ecol. Manage.* **352** 9–20

Lawrence D and Vandecar K 2014 Effects of tropical deforestation on climate and agriculture *Nat. Clim. Change* **5** 27–36

Li Y, Zhao M, Motesharrei S, Mu Q, Kalnay E and Li S 2015 Local cooling and warming effects of forests based on satellite observations *Nat. Commun.* **6** 6603

McAlpine C A, Johnson A, Salazar A, Syktus J, Wilson K, Meijaard E, Seabrook L, Dargusch P, Nordin H and Sheil D 2018 Forest loss and Borneo's climate *Environ. Res. Lett.* **13** 044009

McAlpine C, Syktus J, Ryan J, Deo R, McKeon G, McGowan H and Phinn S 2009 A continent under stress: interactions, feedbacks and risks associated with impact of modified land cover on Australia's climate *Glob. Change Biol.* **15** 2206–23

McIntosh P C and Hendon H H 2018 Understanding Rossby wave trains forced by the Indian Ocean Dipole *Clim. Dyn.* **50** 2783–98

Myneni R, Knyazikhin Y and Park T 2015 MOD15A2H MODIS/terra leaf area index/FPAR 8 day L4 global 500 m SIN grid V006 *NASA EOSDIS Land Processes DAAC*

Ordway E M, Asner G P and Lambin E F 2017 Deforestation risk due to commodity crop expansion in sub-Saharan Africa *Environ. Res. Lett.* **12** 044015

Riccobono F et al 2014 Oxidation products of biogenic emissions contribute to nucleation of atmospheric particles *Science* **344** 717–21

Salazar A, Baldi G, Hirota M, Syktus J and McAlpine C 2015 Land use and land cover change impacts on the regional climate of non-Amazonian South America: a review *Glob. Planet. Change* **128** 103–19

Scheffer M, Carpenter S, Foley J A, Folke C and Walker B 2001 Catastrophic shifts in ecosystems *Nature* **413** 591–6

Semazzi F H and Song Y 2001 A GCM study of climate change induced by deforestation in Africa *Clim. Res.* **17** 169–82

Spracklen D V and Garcia-Carreras L 2015 The impact of Amazonian deforestation on Amazon basin rainfall *Geophys. Res. Lett.* **42** 9546–52

UN 2019 World Population Prospects 2019 (New York: United Nations Department of Economic and Social Affairs)

Van Ittersum M K et al 2016 Can sub-Saharan Africa feed itself? *Proc. Nat Acad. Sci. USA* **113** 14964–9

Van Noordwijk M and Ellison D 2019 Rainfall recycling needs to be considered in defining limits to the world's green water resources *Proc. Nat Acad. Sci. USA* **116** 8102–3

Virtanen P, Gommers R, Oliphant T E, Haberland M, Reddy T, Cournapeau D, Burovski E, Peterson P, Weckesser W and Bright J 2020 SciPy 1.0: fundamental algorithms for scientific computing in Python *Nat. Methods* **17** 261–72

Wang-Erlandsson L, Fetzer I, Keys P W, Van Der Ent R J, Savenije H H G and Gordon L J 2018 Remote land use impacts on river flows through atmospheric teleconnections *Hydrol. Earth Syst. Sci.* **22** 4311–28

Shi X, Chen Z, Wang H, Yeung D-Y, Wong W-K and Woo W-C 2015 Convolutional LSTM network: A machine learning approach for precipitation nowcasting *Montreal, Canada* 2015-January *29th Annual Conference on Neural Information Processing Systems, NIPS 2015* pp 802–10

Zeng N 2003 Atmospheric science. Drought in the Sahel *Science* **302** 999–1000

Zheng X and Eltahir E A 1997 The response to deforestation and desertification in a model of West African monsoons *Geophys. Res. Lett.* **24** 155–8